RF cavity passive wireless sensors with time domain gating based interrogation for SHM of civil structures

D.J. Thomson, D. Card and G.E. Bridges

Department of Electrical and Computer Engineering

University of Manitoba, Winnipeg, Canada

Abstract

Many existing sensing technologies for application to the monitoring of large systems or civil structures have a serious deficiency in that they require some type of wired physical connection to the outside world. This causes significant problems in the installation and long term use of these sensors. This paper describes a new type of passive wireless sensor that is based on resonant RF cavities, where the resonant frequency is modulated by a measurand. In the case of a strain sensor, the electrical length of the cavity directly modulates it's resonant frequency. A probe inside the cavity couples RF signals from the cavity to an externally attached antenna. The sensor can then be interrogated remotely using microwave pulse-echo techniques. Such a system has the advantage of requiring no permanent physical connection between the sensor and the data acquisition system. In this type of sensor the RF interrogation signal is transmitted to the sensor and then re-radiated back to the interrogator from the sensor resulting in a signal strength that decreases with the forth power of distance. This places an upper limit

on the distance over which the sensor can be interrogated. Theoretical estimates show that these sensors can be interrogated with sufficient signal-to-noise ratio at distances exceeding 10 m for radiated powers of less than 1 mW. We present results for a strain sensor and a displacement sensor that can be interrogated at a distance of 8 m with a strain resolution of less than 10 ppm and displacement resolution of 0.01 mm, respectively.

Keywords: wireless sensors, radio frequency, structural health monitoring, passive, resonant cavity

Corresponding author: D.J. Thomson, Thomson@ee.umanitoba.ca

Introduction

Most existing sensing technologies used for the monitoring of large or civil infrastructure have a serious deficiency in that they require a wired physical connection to the outside world. Documented cases have shown that the cost of installation and preparation of sites for monitoring can easily equal the cost of the sensors and interrogation equipment. For example, the cost of installing a monitoring system in the Tsing Ma suspension bridge in Hong Kong was reported to be over $27,000 per sensor channel [1] and the cost of the monitoring system for the St. Anthony Falls Bridge in Minneapolis was reported to be $3,000 per sensor [2]. Wireless sensors are an attractive solution to this problem. However, many types of wireless sensors require battery or local power for electronics on the sensor. This negates many of the advantages of wireless sensors, as the batteries require frequent replacement. Research is progressing on wireless sensors operating from scavenged or radiated power, but it is not yet clear if the accuracy, stability and cost requirements for monitoring civil infrastructure can be met [3-5]. Passive wireless sensors are an emerging alternative, where the sensor is a passive device and hence there is no requirement for local power. Several types of passive wireless sensing systems have been demonstrated. For example, surface acoustic wave (SAW) sensors have been developed for monitoring a number of properties [6,7] and are based on the perturbation of the propagation velocity of acoustic waves by the measurand of interest. Interrogation is most often done through the use of pulse-echo techniques [6,7]. However, SAW sensors suffer from high losses [SAW losses] and it can be difficult to efficiently couple the measurand to the surface acoustic waves within the sensor [6,7]. Magneto-resonant [8,9] and resonant coil

based systems are other methods for measurement of a large number of physical parameters [10,11]. These sensors have proven useful for measuring corrosion [11]. However, magneto-resonant and coupled coil sensors suffer from limited interrogation range (~10 cm) and are not suitable for measuring property changes in the ppm range [12]. This is important for civil SHM where less than 10 microstrain resolution is required for applications such as measuring loss of pre- and post-stress in concrete beams and girders [13,14]. In a previous work we demonstrated a proof-of-concept version of a passive wireless sensor based on resonant RF cavities [15]. In this paper a passive wireless sensor technique is presented that can measure less than 10 ppm resonant frequency changes, and hence less than 10 microstrain resolution, at distances of up to 8m.

Sensor System Operation

The fundamental elements of the RF cavity passive sensor concept are shown in Fig. 1. The sensor is a passive device, often constructed using copper cylinders and a simple antenna as shown in the upper left of Fig. 1. This sensor would be mounted on the surface of or embedded in a structure. If mounted on a girder it could be used to detect the presence of damage such as that shown in the lower right of Fig. 1. The interrogator transmits an RF pulse from an antenna to the antenna on the sensor and then into the cavity. After a specified time the transmitter turns off and the interrogator switches to a receiving mode. The RF cavity sensor emits an echo that contains energy that has been stored in the cavity. The magnitude of this echo, as described below, can be used to make several different types of useful sensors. The advantages of this approach are that batteries are not

required on the sensor and that, due to the high operating frequency, directional antennas can be employed to increase the range beyond what is possible with inductively coupled sensors.

A block diagram of the passive RF cavity based sensing system is illustrated in Fig. 2. The sensor has only one RF input-output port. It is interrogated by first sending a signal to excite the resonator and subsequently detecting the reflected or re-radiated signal. There are many ways to interrogate the resonant frequency of the sensor. We have chosen a time-domain gating approach that starts with the transmission of a pulse-modulated RF signal from the interrogation system to the sensor where it excites an electromagnetic field in the cavity. The maximum re-radiated signal will be generated when the RF frequency is selected so that the incoming signal is most efficiently coupled to the cavity. This frequency will be close to the resonant frequency of the cavity. The initial transmitted signal is maintained until the field in the cavity reaches equilibrium. For a typical sensor example with a resonant frequency of approximately 2.4-2.5 GHz and a Q greater than 2000, equilibrium will occur in approximately 400 ns. After equilibrium is reached, the input signal is switched off and the stored energy will re-radiate out of the resonator as a decaying RF signal. The interrogation unit now acts as a receiver and the re-radiated signal is directed through an amplifier into a RF detector such that the power of the re-radiated signal can be measured. A second gating switch, with a delay after the transmission is turned off, is used to eliminate the effects of unwanted reflections from objects in the environment [7,16]. Since objects in the environment are not generally resonant, their reflections can be greatly reduced with this second switch. Typically a delay of 100 ns is used. This has a small effect on the signal received

from the sensor, which is highly resonant. To determine the resonant frequency of the cavity the transmitted RF signal is swept over a range of frequencies to find the frequency at which the power received at the detector is a maximum.

With any wireless sensor one important parameter is the distance over which the sensor can be used. In this paper we derive a theoretical estimate for the maximum distance over which a passive RF cavity sensor can be interrogated and will present results of measurements made at distances up to 8 meters. Results from two sensors developed for applications to structural health monitoring of civil structures are presented. The first is a strain sensor with microstrain resolution. This sensor can also be used to sense temperature induced strain and results will be presented using it as a temperature sensor. The second is a displacement sensor with a sensing range of ~2 mm and a resolution of 0.01 mm. This sensor has application in SHM of civil structures for crack width monitoring, which research suggests is an indicator of fatigue in concrete bridge decks [17,18].

Theoretical Estimates of the Maximum Sensor Interrogation Distance

For a passive RF cavity sensor (RFCS), the maximum sensor interrogation distance can be estimated through the ratio of the transmitted to received power and the minimum required signal-to-noise ratio of the receiver. Since the sensor acts as a scattering object, the radar equation can be used to estimate the transmit-to-receive power ratio at the receiver. For a system operating at a free-space wavelength, λ, where the interrogator antenna has gain, G_i , and the sensor antenna has gain, G_s , and they are separated by a distance R

$$\frac{P_r}{P_t} = \frac{G_s^2 G_i^2 \lambda^4}{(4\pi R)^4} \frac{1}{D\Gamma} \quad . \tag{1}$$

Here P_t is the power transmitted by the interrogator towards the RFCS, P_r is the power received back at the interrogator and Γ is the return loss of the sensor attached to the sensor antenna. For a passive RFCS, $D\Gamma$ represents the ratio of energy received by the sensor to the energy re-transmitted during an interrogation cycle and includes loss due to the interrogator duty cycle. Typically, $D\Gamma$ ranges from 1/0.3 to 1/0.1. Equation 1 assumes free space transmission. Equation 1 can easily be modified to include other losses due to walls or concrete, for embedded sensors, and would reduce the received power [19]. The minimum detectable signal at the receiver is

$$P_r = P_{\min} = kTB \cdot F \cdot SNR \quad , \tag{2}$$

where kT is thermal energy, B is the bandwidth of the receiver, F is the noise figure of the receiver and SNR is the required signal-to-noise ratio of the receiver. The maximum distance at which the sensor can be interrogated is then given by [6]

$$R_{\max} = \frac{\lambda}{4\pi} \left(\frac{P_t G_s^2 G_i^2}{SNR \cdot kTB \cdot F \cdot D\Gamma} \right)^{1/4} \quad . \tag{3}$$

The required signal-to-noise ratio is determined by the receiver and detection method used to find the resonant frequency of the RFCS to a desired resolution.

The frequency measurement resolution is obtained by determining the interrogator signal as a function of change in the resonance frequency, Δf_r, of the RFCS sensor due to a change in the parameter being measured. Consider the frequency response of a typical resonator as shown in Fig. 3, where Q is the quality factor and f_r is the resonant frequency. The interrogator finds the resonant frequency by measuring the response at two frequencies, $V_1=V(f_1)$ and $V_2=V(f_2)$. The interrogator signal is the difference between these, $v_s=V_2-V_1$, and will be zero when f_1 and f_2 are symmetrically spaced about the resonant frequency, $f_r=f_0$. If the resonant frequency changes, $f_r=f_0+\Delta f_r$, due to a change in the parameter being measured, the signal will be,

$$v_s = \left[V_2\big|_{f_r=f_0+\Delta f_r} - V_1\big|_{f_r=f_0+\Delta f_r} \right] \cong 2\left.\frac{dV}{df}\right|_{f_1} \Delta f_r \quad , \tag{4}$$

assuming a small change in frequency, $\Delta f_r << f_r /Q$, and a symmetrical frequency response. For a high-Q second-order resonator, the dV/df term above is maximized when we choose $f_{2,1} = f_r \pm f_r /(\sqrt{8}Q)$. The interrogator signal in this case is [15]

$$v_s\big|_{f_r=f_0+\Delta f_r} = 2\left.\frac{dV}{df}\right|_{f_r - f_r/\sqrt{8}Q} \Delta f_r = V_{\max}\left(\frac{8Q}{3\sqrt{3}f_r}\right)\Delta f_r \quad , \tag{5}$$

where $V_{max} = V(f_r)$. is the maximum detector output at resonance.

Assuming the noise voltage in each measurement is v_N, we can estimate the minimum measurable change in resonant frequency $f_r|_{min}$ by equating the noise voltage to the signal v_s so that

$$\delta f_r = \Delta f_r\big|_{\min} = V_{\max}\left(\frac{3\sqrt{3}f_r}{8Q}\right)\frac{v_N}{V_{\max}} \quad . \tag{6}$$

The frequency measurement resolution of the sensor system, δf_r, can then be related to the SNR of the receiver, $SNR = V_{max}/v_N$, as

$$SNR = \left(\frac{3\sqrt{3}}{8Q}\right)\frac{f_r}{\delta f_r} \quad . \tag{7}$$

For example consider a typical RFCS, with a Q = 1000 and operating at f_r=2500 MHz (within the ISM band), and used for strain monitoring applications in civil infrastructure [15]. A linear RFCS sensor would produce a frequency shift of 2.5 kHz/microstrain. A desired 5 microstrain resolution would require a frequency resolution of δf_r = 12.5 kHz and, from equation 7 above, require an interrogator system SNR = 130. With the required SNR now specified for a particular application, we can then use equation 3 to find an estimate for the maximum interrogation distance. For example, for a transmitted power P_t=1 mW, kT= $4X10^{-21}$ J, B = 10 kHz, receiver noise figure F = 1 dB, a sensor return loss DΓ = 10 dB (This would include loss due to the duty cycle of the interrogator gating),

interrogator and sensor antenna gains G_i = 10 dB and G_s = 10 dB and wavelength λ = 0.12, the maximum monitoring distance would be R_{max} = 42 m.

A useful design chart, Fig. 4, can be produced by using equation 1 to calculate the transmit-to-receive power ratio (or round trip loss) versus distance as a function of antenna gain factors. The maximum allowable loss, assuming a 1 mW transmitted power and a SNR=100, yields a theoretical limit as shown.

It is interesting to note that for all antenna combinations, microstrain (ie. ppm) resolution should be achievable at distances up to 10 m. For appropriate combinations of antennas, such as high interrogator gain, distances up to 30-40 m should be possible. Many different types of antennas can be employed depending on the sensor application. We have used lower gain conformal microstrip patch antennas (see Fig. 1) and higher gain commercial antennas (described below) suited to externally mounted antenna applications. For sensors embedded in concrete, covered microstrip antennas have been designed and shown to have a gain of –5dB, this including both transmission and mismatch losses due to the concrete [20]. To test the theoretical estimates experiments were conducted with sensors at various distances using an interrogation system developed for the RFCS sensors.

Interrogation System for Wireless Sensing

A photograph of the interrogation system is shown in Fig. 5. The interrogation process starts with the transmission of an RF signal from the source (National Semiconductor LMX2470). This signal is passed from the signal generator to the

transmitting antenna via a switch (Minicircuits ZASWA-2-50 RF switch). The transmitted signal then energies the sensing cavity. For this resonator with a frequency of approximately 2.41 GHz and Q approximately 1000, equilibrium of the excited field will occur in approximately 400 ns. 500 ns after equilibrium is reached the interrogation unit switches from send to receive. The energy stored in resonator will re-radiate out from the resonator and out of the attached antenna in the form of a decaying RF signal. The received signal is directed through a low noise amplifier (LNA) into an RF detector (Analog Devices AD8347 evaluation board), which produces a voltage proportional to the incoming signal power. This voltage is then digitized using an A/D and downloaded to a laptop for processing. A second switch (see Fig. 2) was used in the interrogation system to reduce the effects of environmental reflections and noise on the detected signal [16]. This switch has a 100 ns delay time and will eliminate signals reflecting from objects up to 15 m from the transmitting antenna. This technique has been employed successfully in the past with SAW based sensors in reducing environmental reflections [7].

By sweeping through a range of frequencies and monitoring the signal after low pass filtering the resonant peak can be easily located. Fig. 6 shows a typical result obtained by sweeping through the resonant peak of a strain sensor at various distances between the interrogation system antenna and the sensor antenna. Clearly, the peaks can be easily identified and the background signal is low and relatively constant. The background is believed to be due to coupling within the interrogation system. Once the swept-frequency data is obtained one then has to determine the

location of the peak in the presence of electronic and other forms of noise. In this work a servo peak location algorithm was employed [21].

The servo algorithm uses a frequency sweep to find a coarse estimate for the peak position and peak magnitude [21]. Then the signal is sampled at frequencies above and below the estimated peak frequency (a difference frequency of1 MHz for this example). The difference between the two samples is calculated. If the peak is exactly half way between the two samples and the peak is symmetric then the difference will be 0. If the difference is not zero it is used to find a better estimate of the peak. The process is repeated for a certain number of iterations or until peak position is determined to the required resolution. This algorithm has been found to be stable and yield estimates of peak position that are significantly less than the frequency bandwidth at the peak (less than 10 kHz in the present case) [21].

To test the ultimate limits of the sensor system, measurements were made on a roof-top away from the RF noise due to local area network (LAN) and other wireless communication activity. Fig. 7 shows a photograph of the set up for these tests. For distances greater than 4.4 m as shown in the photograph the tests were carried out horizontally. In these tests a 16 dB gain antenna was used with the interrogator and a 10 dB gain antenna was used with the sensor (Superpass SPAPG16 and SPAPG10). The radiated power was approximately 1 mW. The sensor response versus frequency was measured at distances from 1.9 m to 7.9 m. The results of these tests are shown in figure 8. Up to 7.9 m the resonant peak can be clearly resolved and the signal-to-noise ratio is above 100:1 or greater.

Strain and Temperature Sensors

The wireless strain sensing system consists of a passive resonant cavity sensor that is embedded in the structure, and a portable interrogator. An antenna that is attached to the sensor will receive the signals and couple them into the sensor cavity, which will absorb energy in a narrow frequency band, as determined by the cavity's dimensions. When the transmitted signal is turned off, the cavity will reemit energy back to the interrogator, which uses the information received to calculate strain on the sensor. A diagram illustrating how the wireless strain sensor functions is shown in Fig. 9.

Theoretical Basis of Sensor

A schematic diagram of the sensor is shown in Fig. 9. There are many types of electromagnetic cavities with resonant frequencies that change with dimension. The strain sensor we have employed as a simple coaxial cavity with length *l*. A small wire probe extends into the cavity at it's center to excite the electromagnetic field. The cavity can support many possible resonant modes, the dominant mode (and lowest resonant frequency) being the TEM mode, where the field is a maximum at the center of the cavity and zero at the ends [22]. The TEM resonant frequency is

$$f_r = \frac{c}{2l\sqrt{\varepsilon_r}} \tag{8}$$

where c is the speed of light in vacuum and ε_r is the relative permittivity of the material filling the coaxial cavity (in our case air, $\varepsilon_r \sim 1$). When the structural material in which the sensor is encased or attached is stressed it will force a change

in dimensions of the cavity. The longitudinal dimensional change, Δl, will result in a shift in resonant frequency that can be used to unambiguously determine the strain, Δl/l, in the structure. If the elastic properties of the sensor material differ from the material in which it is embedded or to which it is attached, a gauge factor may be required. For small strains, Δl « l, the shift in resonant frequency can be approximated as

$$f_{strained} = \frac{c}{2(l + \Delta l)} = \frac{c}{2l}\left(\frac{1}{1+\varepsilon}\right) \approx f_{unstrained}(1-\varepsilon) \tag{9}$$

$$\Delta f_r = f_{strained} - f_{unstrained} \approx -f_{unstrained}\varepsilon \tag{10}$$

where ε = Δl/l is the strain. Typically the structure is under compression resulting in a positive shift in frequency.

As long as the unstrained resonant frequency is known then the strain can be determined with the same accuracy as the resonant frequency can be measured. One advantage of this approach is that RF signals can be generated with very high accuracy and stability. RF signal generating sources can be frequency locked to quartz crystal oscillators, which are easily obtained with errors of less than one part-per-million and stability within a few parts-per-billion [23].

The sensors were constructed from 25.4 mm diameter copper tubing with a wall thickness of 2.5 mm. The end caps were machined from solid copper. The center conductor was solid copper and 6.3 mm in diameter. The pieces were soldered

together to form the cavity. A hole was drilled and tapped into the side of the cavity to accept an SMA-type coaxial RF connector which had it's center conductor extended by 4 mm to act as a wire probe. The SMA connector was inserted into the cavity and positioned so that an input return loss in the range of 5 to 10 dB was obtained.

To demonstrate the frequency stability that is possible with this approach a strain sensor of the type described was interrogated over several hours, while efforts were made to keep temperature stable, to reduce the effects of thermal induced strain. Fig. 10 shows measurements of the frequency shift over several hours. Each frequency sweep took ~7 seconds and from each sweep a maximum was estimated. Thirty of these maximums were averaged to produce each point on the plot in Fig. 10. Over the several hours monitored the total drift was less than 7 parts per million (ppm). The sensor was made of copper and this could be due to a temperature induced strain drift for a sensor temperature drift of 0.43 C over that time. The plot also has spikes that may be due to RF interference from local area networks or signals from other wireless devices. The plot also has resonant frequency shifts that appear to be quantized. These may be due to the quantization of the frequency source. In this example the minimum step size for the source was 10 kHz. Even though the signal is averaged over many frequency locations, it is possible that the quantization of the source may result in quantization of the estimated resonant frequency.

The theoretical estimates for RF cavity sensors conclude that ppm resolution measurements should be possible at distances of up to 10 m. To test this prediction resonant frequency measurements have been made on an unstrained cavity at distances up to 10 m. The sensing cavity was placed a distances from 1 to 10 m from the interrogator antenna. The resonant frequency of the cavity was then measured using the techniques outlined above. The measurements shown in Fig. 11 are referenced to the 1 m measurement. At each distance 10 measurements were made and the standard deviation was estimated from the 10 measurements. At distances of 8 m or less the standard deviation is less than 7 ppm. This is in agreement with the calculations above that would predict that the SNR should be in excess of the 130 required to achieve less than 10 ppm resolution. Fig. 11 indicates that for distances greater than 9 m the error exceeds 15 ppm. The result for 9 m is greater than predicted theoretically. Coupling from the RF source to the receiver results in a background signal that may contribute to this deviation. The absolute strain also deviates from theoretical expectations even though it is expected that the strain measurement would not deviate more that the standard deviation. At all distances beyond 1 m the measured strain differs from the strain measured at 1 m by more that the standard deviation. Therefore, other contributions to the measurement uncertainty that are greater than the random variation of the signal are evident. One source we have identified is due to the path length sensitivity of the measurement. In measurements not shown, the measured strain was observed to vary periodically over a half wavelength as the distance to the sensor was changed in small increments. This effect may be due to phase sensitivity in the detector.

Strain can be changed in the sensor by many means. Temperature will change strain due to thermal expansion or contraction. Thermal induced strain can be used to measure temperature or could be used a means to measure temperature so that temperature induced strain could be isolated from other sources of strain. Temperature induced strain was measured in a copper co-axial cavity resonator sensor as described above. The sensor was put into and environmental chamber and a thermocouple was attached to the outer surface of the cavity. The temperature of the chamber was ramped from room temperature to ~+150C, then slowly cooled down to +35C. During the temperature cycle the sensor was wirelessly interrogated and resonant frequency measurements were taken continuously. At room temperature copper has a thermal expansion coefficient of 16.3 ppm/C [24]. For a coaxial resonator operating at 2.45 GHz this would result is a frequency shift of 39.9 kHz/C. Results of this test are shown in Fig. 12 with results referenced to 40C. The wireless sensor tracks the thermocouple over the range of temperatures used. However, deviations can be seen at some temperatures, such as 120C. At this temperature the wireless sensor deviates from the thermocouple by more the 1.5C. This could be due to path length sensitivity discussed above.

Displacement Sensor

In a displacement sensor displacement must be converted into a signal format that can be used for observation or measurement. The sensor described here uses a non-TEM mode electromagnetic cavity to covert displacement to frequency. A hollow conducting cavity can have an infinite number resonant electromagnetic modes. For the displacement sensor we have chosen a cylindrical cavity for reasons of ease of

fabrication. The sensor is shown in Fig. 13 and consists of a rigid cylindrical cavity with a flexible diaphragm at one end of the cylinder. A metal rod is attached to the cavity diaphragm. As the rod is linearly displaced it causes the diaphragm to deflect, this changing the dimensions of the cylindrical cavity, resulting in a shift in the cavity resonant frequency. The resonant frequency for the dominant TE_{111} mode of a hollow cylindrical cavity is

$$f_r = \frac{c}{2\pi}\sqrt{\left(\frac{1.841}{d/2}\right)^2 + \left(\frac{\pi}{l}\right)^2} \tag{11}$$

where d is the diameter and l is the length of the cylinder [23]. For a desired resonant frequency there is a trade-off between d and l, with a smaller length providing better strain sensitivity at the expense of a larger diameter. The TE_{111} mode is efficiently excited using a wire probe inserted into the side-wall of the cylinder as shown in Fig. 13.

The cavity we employed for displacement sensing was fabricated from 100 mm diameter copper tubing and is 88 mm long with a thickness of 2.5 mm. The back plate and the bracket were welded together. The corrugated diaphragm was fabricated from brass sheet and hydraulically formed using machined dies and was soldered to the copper cavity. An SMA connector with a center conductor wire probe extending approximately 5 mm into the cavity provided an input return loss of ~ 5 to 10 dB. When the rod in Fig. 13 is displaced there is a shift of the cavity resonant frequency.

The displacement sensor was characterized using a test fixture employed for the calibration of linear displacement sensors. A precision micrometer was used to translate a wire attached to the diaphragm of the displacement sensor as shown in Fig. 14. The diaphragm was slightly preloaded (~0.5 mm) to avoid having a dead band and the sensor was displaced in 0.1 mm increments. The uncertainly in the displacement produced by the test fixture is estimated to be less than 0.01 mm. At each displacement increment a coarse sweep of frequency is made and then 30 iterations of the servo algorithm are employed so that the measurement takes about 7 seconds per increment. The resonant frequency for the first displacement measurement was used as a reference point to produce a plot of resonant frequency shift versus displacement as presented in Fig. 15. For a total displacement of 2 mm the resonant frequency shifted by 14 MHz. The shift is close to linear and the proportionality constant is 7 MHz/mm. The maximum deviation from linearity was 0.06 mm over the 2 mm range. The uncertainty for this particular measurement is less than 0.06 MHz, providing a resolution better than 0.008 mm. This is less than the uncertainty in the displacement test fixture of 0.01 mm. In a controlled environment these measurements have been taken at distances of up to 4.5 m between the interrogator and the sensor antennas.

DISCUSSION AND CONCLUSIONS

A sensing system based on RF resonant cavity sensors that are interrogated by gated RF signals has been presented. Theoretical calculations predict that these sensors can be interrogated at distances of over 10 m while being capable of

resolving less than 10 ppm shift in resonant frequency. To achieve this resolution a SNR of 130 or greater is required. . The use of these sensors for measuring strain, temperature induced strain and displacement has been demonstrated. Strain resolution of less than 10 ppm is possible at a range of 8 m and displacement resolution of less than 0.01 mm is possible at 4.5 m. Passive wireless sensors based of resonant RF cavities should find application in monitoring of civil infrastructure.

REFERENCES

1. Xia, Y., Aoki, S., Abe, M., Fujino, Y.,"A Remote Intelligent Monitoring System (RIMS) for Infrastructures", Proc. 1st International Conference SHMII, Tokyo, Nov. 13 – 15, 2003, A. A. Balkema Pub., pp 359 – 363
2. Hamm S.,"The bridge to smart technology", Business week, February 19, 2009
3. Calhoun B.H., Daly D.C., Verma N., Finchelstein D.F., Wentzloff D.D., Wang A., Cho S.H., Chandrakasan A.P., "Design considerations for ultra-low energy wireless microsensor nodes", IEEE Tran. on Computers, Vol. 54, No. 6, pp. 727-740, 2005
4. Le T, Mayaram K and Fiez T , "Efficient far-field radio frequency energy harvesting for passively powered sensor networks", IEEE J. of Solid-state Circuits, Vol. 43, No. 5, pp. 1287-1302, 2008
5. A. P. Sample, D.J. Yeager, P. S. Powledge, and J.R. Smith, "Design of a Passively-Powered, Programmable Sensing Platform for UHF RFID Systems", Proceedings of the 2007 IEEE International Conference on RFID, pp. 149-156, Grapevine, TX, USA, March 26-28, 2007

6. Wolf-Eckhart Bulst, Gehard Fischerauer, Leonhard Reindl, “State of the art in Wireless sensing with surface acoustic waves”, IEEE Trans. Indus. Elec., Vol. 48, Iss. 2, pp. 265-271, 2001
7. Pohl A, “A review of wireless SAW sensors”, IEEE trans. Ultrasonics Ferroelectrics and frequency control, Vol. 47, No. 2, pp. 317-332, 2000
8. Jain MK, Grimes CA , “A wireless magnetoelastic micro-sensor array for simultaneous measurement of temperature and pressure” , IEEE Trans. on Magnetics, Vol. 37, No. 4, pp. 2022-2024, 2001
9. Grimes C.A., Mungle C.S., Zeng Z.F., Jain M.K., Dreschel W.R., Paulose M., Ong K.G.,”Wireless magnetoelastic resonance sensors: A critical review”, SENSORS, Vol. 2, Iss. 7, pp. 294-313, 2002
10. Butler J.C., Vigliotti A.J., Verdi F.W., Walsh S.M.,”Wireless, passive, resonant-circuit, inductively coupled, inductive strain sensor”, Sensors and Actuators A, Vol. 102, Iss. 1-2, pp. 61-66, 2002
11. M. M. Andringa, J. Puryear, D. P. Neikirk, S. L. Wood,”Low-cost wireless corrosion and conductivity sensors”, SPIE Smart Structures and Materials for Health Monitoring and Diagnostics,Paper# 6174-31,San Diego, USA, Mar., 2007
12. Ong K.G., Grimes C.A., Robbins C.L., Singh R.S.,” Design and application of a wireless, passive, resonant-circuit environmental monitoring sensor”, Sensors and Actuators A, Vol. 93, Iss. 1, pp. 33-43, 2001
13. Braimah A, Green M.F., Soudki K.A. , “Long-term behavior of CFRP prestressed concrete beams”, PCI JOURNAL, Vol. 48, No. 2, pp. 98-+ , 2003

14. Barr P.J., Kukay B.M. and Halling M.W., “Comparison of prestress losses for a prestress concrete bridge made with high-performance concrete”, J. of Bridge Engineering, Vol. 13, No. 5, pp. 468-475, 2008
15. Chuang J., Thomson, D.J., Bridges G.E., 2005, “Embeddable wireless strain sensor based on resonant rf cavities”, Rev. Sci. Inst., Vol. 76, #094703
16. J. Chuang, D.J. Thomson and G.E. Bridges, “Noise Reduction in Wireless Strain Sensors”, SPIE Smart Structures and Materials for Health Monitoring and Diagnostics, San Diego, USA, Mar. 6-10, 2005
17. D.Card, D.J. Thomson, G.E. Bridges, R. Edalatmanesh and J. Newhook,”A passive wireless sensor for monitoring cracks in civil structures”, 3rd Intl. Conf. on Structural Health Monitoring of Intelligent Infrastructure, Vancouver, Canada, Nov 13-16, 2007, Paper 186
18. Gaudet, J. and Newhook, J.P. 2006. Salmon River Steel-free Bridge Deck – 10 Year Review of Field Performance. Proceedings of IABMAS'06 - Third International Conference on Bridge Maintenance, Safety and Management, Portugal, IABMAS, Paper 376
19. Rappaport T.S.,”Wireless communications principles and practice”, Chapter 4, Prentice Hall, New Jersey, ISBN 0-13-042232-0, 2002
20. M.F. Rad and L. Shafai, ”Embedded microstrip patch antennas for structural health monitoring applications”, IEEE Intl. Symp. on Antennas and Propagation, San Diego, USA, July 5-12, 2008
21. Hladio, R. Jayas, D.J. Thomson and G.E. Bridges, “Development of a field usable interrogation system for RF cavity wireless sensors”, Proc. 3rd Intl.

Conf. Bridge Safety and Management, Porto, Portugal, July 2006, pp. 1001-1003 Paper #381

22. D.M. Pozar, "Microwave Engineering" 3rd ed, Wiley, 2005
23. Lewis L.L., "An introduction to frequency standards", Proceedings of the IEEE, Vol. 79, No. 7, pp. 927-935, 1991
24. NIST/SEMATECH e-Handbook of Statistical Methods http://www.itl.nist.gov/div898/handbook/pmd/section6/pmd64.htm

Figure 1. Passive RF cavity sensors are mounted on or embedded with structures. A sensor with antenna is pictured in the upper left hand corner. The sensor is approximately 90 mm in length. The sensor is interrogated using a pulse/echo technique. The sensor is passive and does not require any local power, such as a battery.

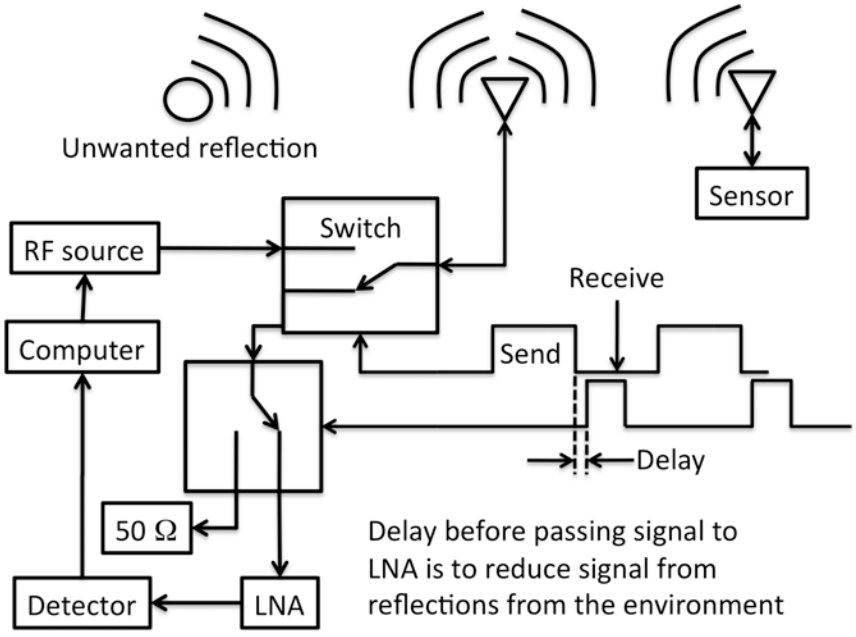

Figure 2. Schematic of the wireless sensing system based on resonant RF resonant cavity sensors.

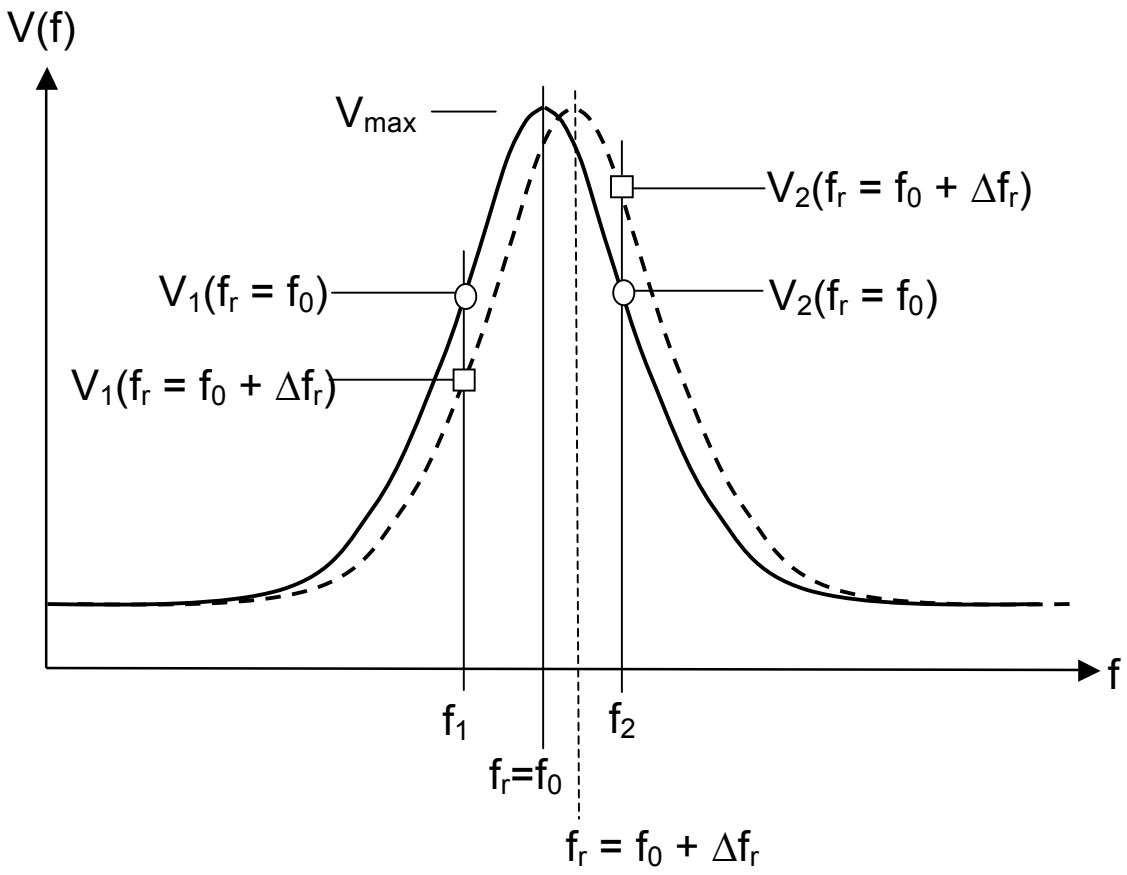

Figure 3. Detected receiver frequency response for a RFCS sensor and showing its change for a shift in resonance frequency due a change in a measured parameter.

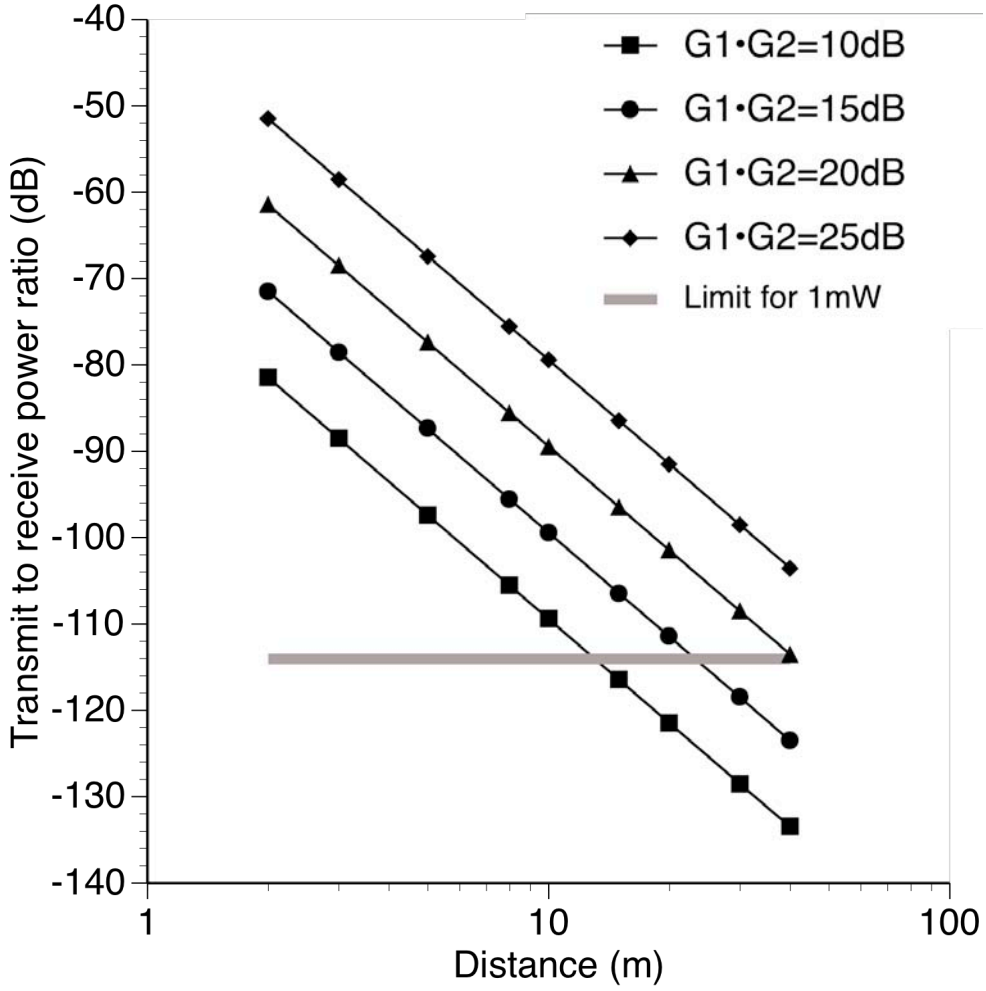

Figure 4. Plot of the transmit-to-receive power ratio for various transmitter and receiver antennas versus distance. The horizontal line at -114 dB is the theoretical limit estimated using equation 3 assuming a transmitted power of 1 mW, kT= $4X10^{-21}$ J, B = 10 kHz, NF = 1, DΓ = -10 dB (this would include loss due to duty cycle and return loss of the sensor), and wavelength = 0.13 m.

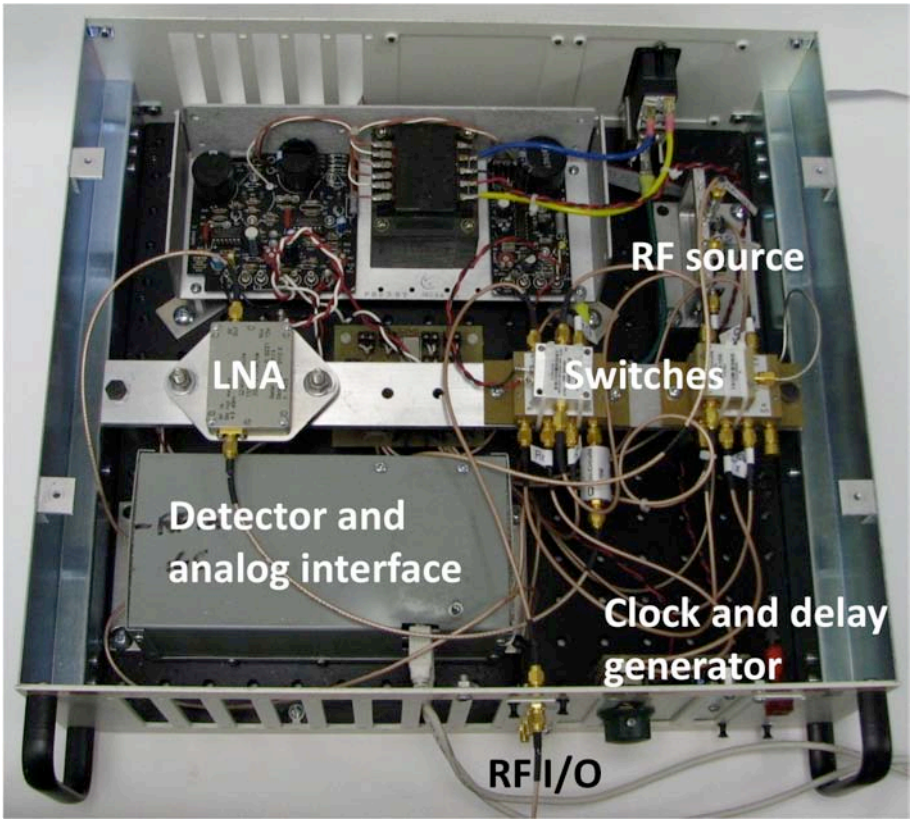

Figure 5. Photograph of the interrogation system. The cabinet is a standard 19 inch rack 15 cm high.

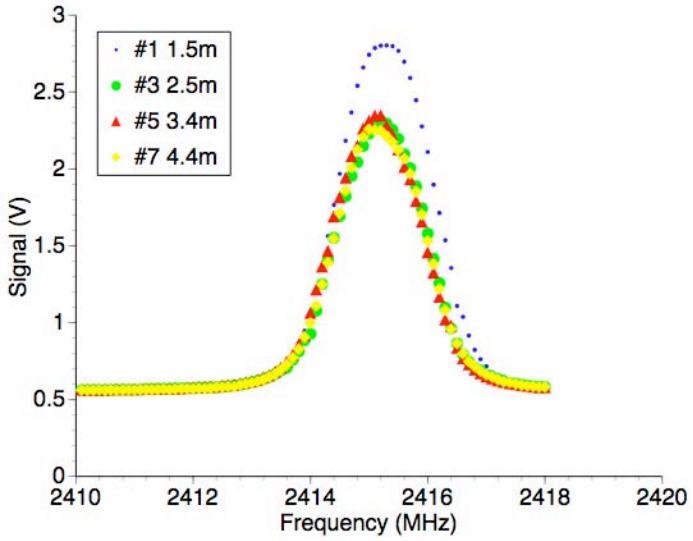

Figure 6 Plot of the response of the strain sensor taken at different distances between the transmitting and receiving antennas. An automatic loop adjusts the gain so that the peak signal strength is approximately equal.

Figure 7 Set up for wireless sensor tests at various distances. The interrogator antenna is on top of the electronics box at the bottom. The sensor is held by an aluminum cable with the antenna at the bottom.

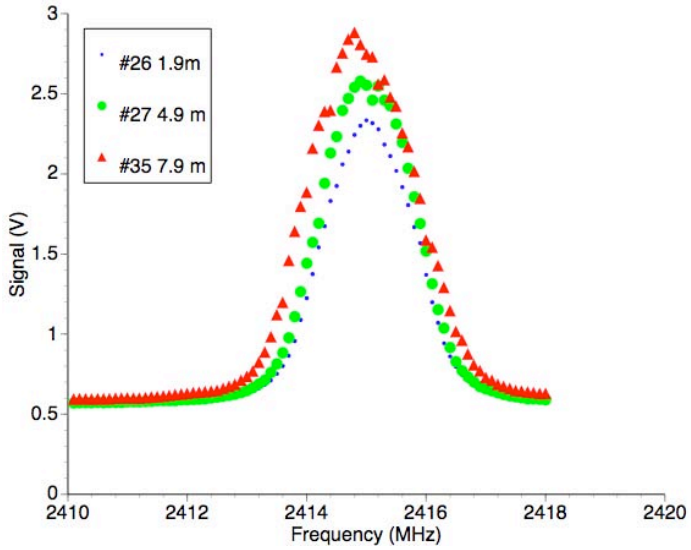

Figure 8 Resonant peaks measured at several distances. Even at the greatest distance of 7.9 m the signal-to-noise ratio is reasonable and the peak is easily identified. The signal-to-noise is estimated to be above the 100:1 required to measure strain with microstrain resolution.

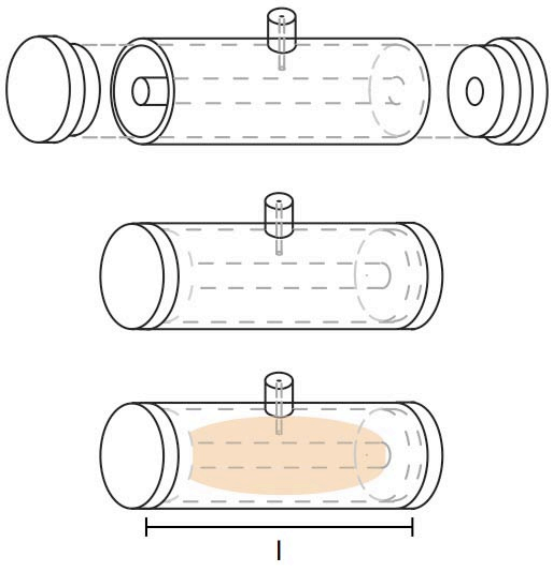

Figure 9. Illustration showing basic construction process and internal field (bottom) of a wireless strain sensor. The sensor was fabricated from 25 mm diameter copper tubing and copper end plates. A 6.3 mm copper rod is positioned in the centre and the assembly is soldered together. An SMA connector-wire probe is used to couple signals.

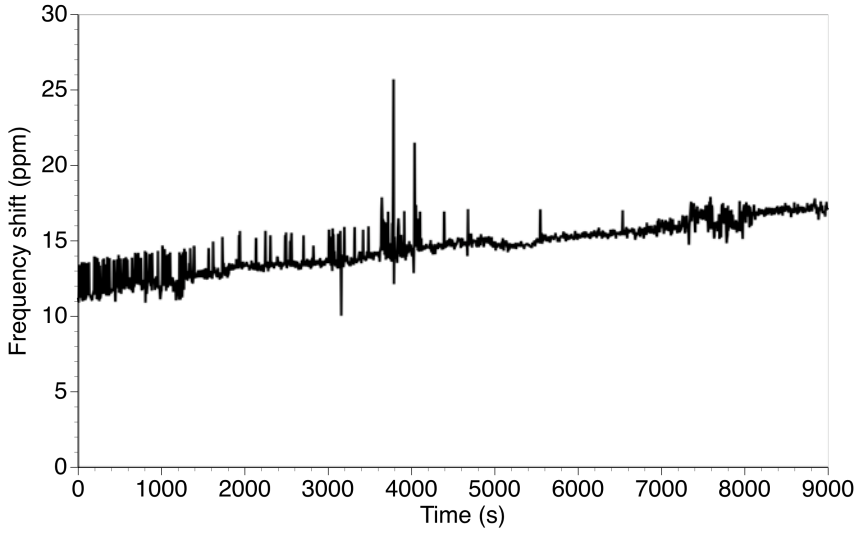

Figure 10. Measurement of frequency drift over several hours. Each frequency sweep took ~7 seconds and from each sweep a maximum was estimated. Thirty maximums were averaged to produce each point on the plot.

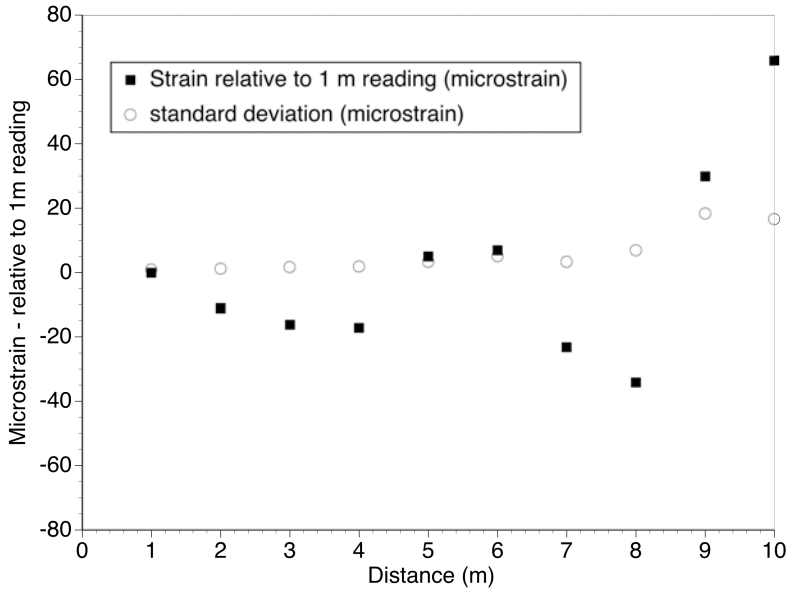

Figure 11. Measured strain in an unstrained sensor as a function of distance to the sensor. As expected the noise and hence the standard deviation of the measurements increases with increasing distance. However, the strain readings deviate by an even larger degree, suggesting other contributions to the measurement uncertainty.

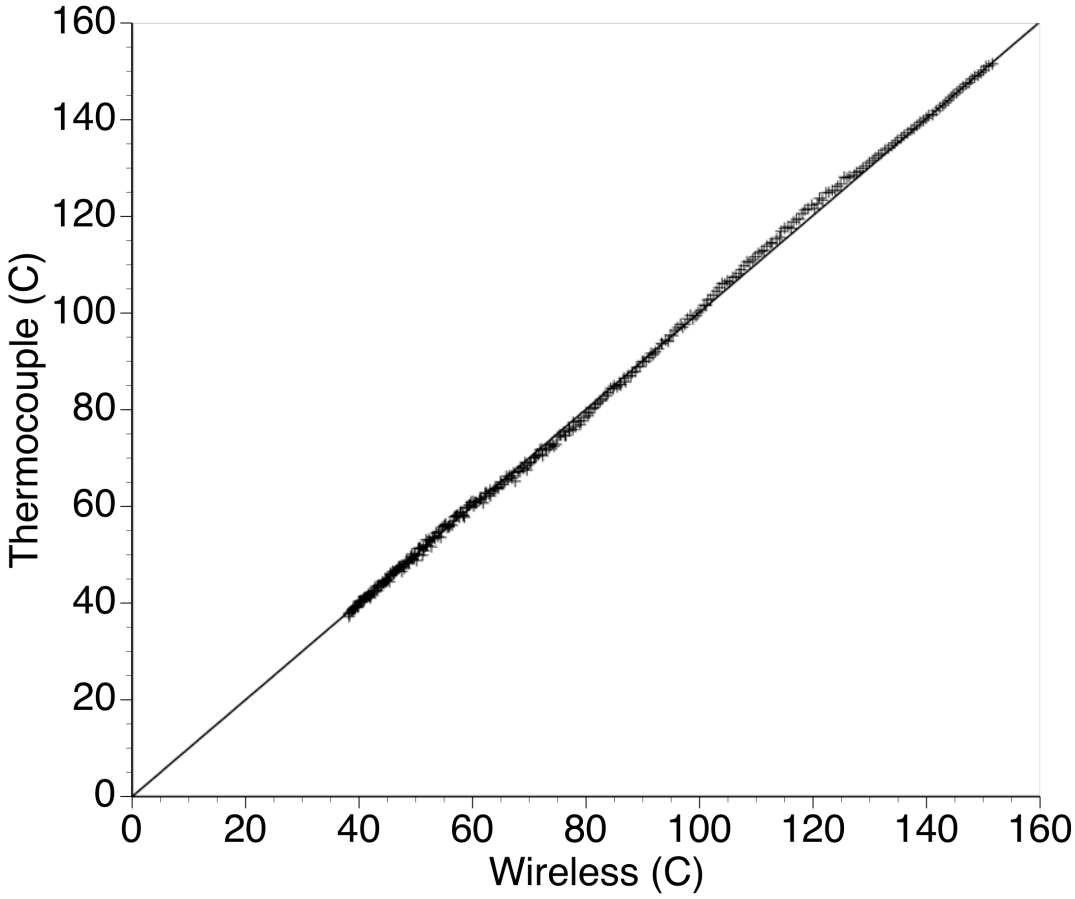

Figure 12. Comparison of temperature measured with wireless sensor versus temperature measured with thermocouple. Wireless sensor was referenced to 40C.

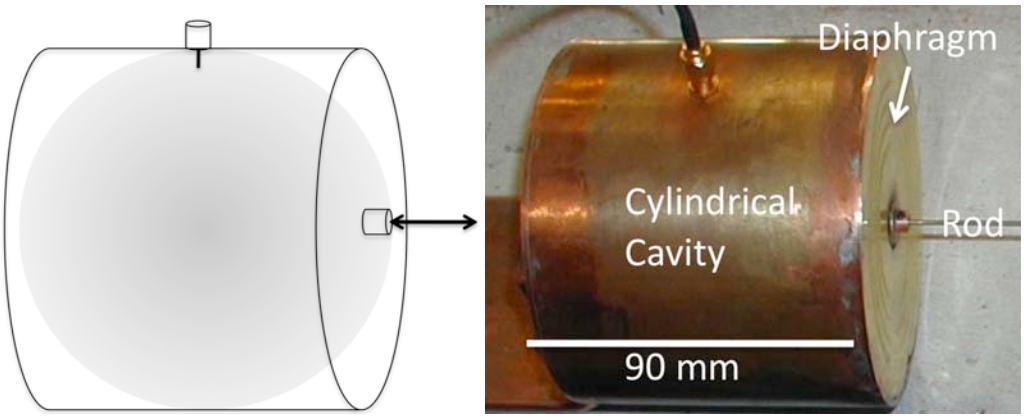

Figure 13. Displacement sensor employing a corrugated diaphragm on one end with a rod attached. As the rod is displaced the diaphragm is displaced causing the cavity to change dimension and hence shift the resonant frequency. The cavity is 100 mm in diameter. An SMA connector-wire probe is used to couple signals in and out of the cavity.

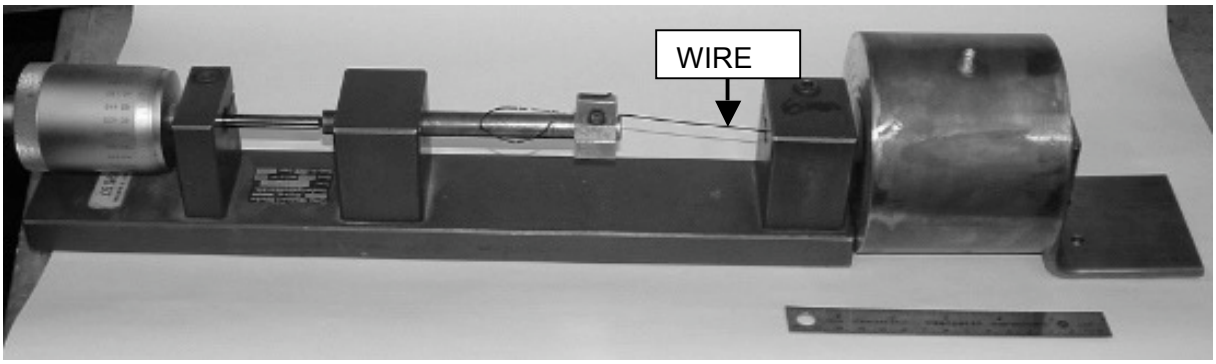

Figure 14. The displacement sensor was mounted on a displacement test fixture and a wire rod was attached to the front of the displacement sensor. Using the micrometer the diaphragm of the displacement sensor was translated in 0.1 mm increments. At each increment the resonant frequency of the cavity was determined using the servo method described.

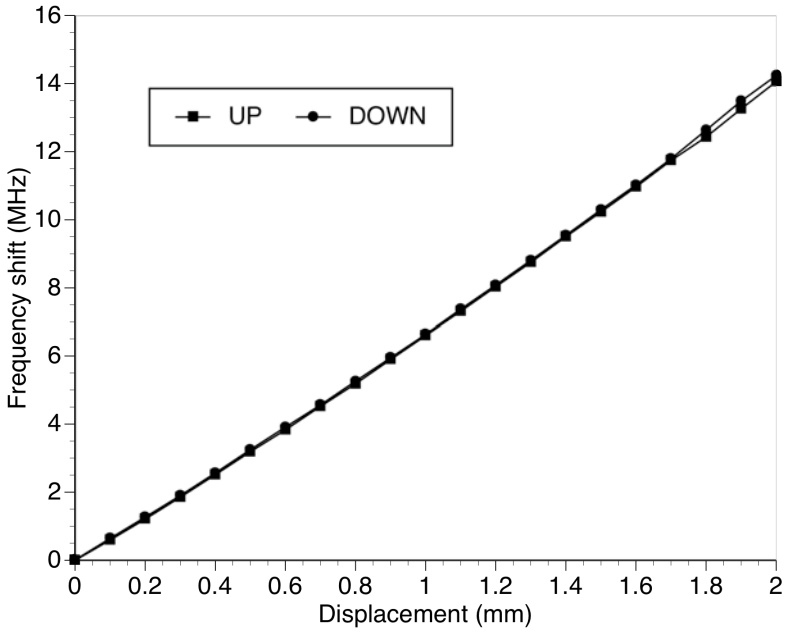

Figure 15. Characterization of resonant frequency shift versus displacement. For a total shift of 2 mm the resonant frequency of the cavity changed by 14 MHz yielding a proportionality constant of 7 MHz/mm. Over the range of these measurements the response of the sensor has a maximum deviation from linearity of 0.06 mm.